ISSN: 2148-9173 Vol: 9 Issue:4 December 2022

International Journal of Environment and Geoinformatics (IJEGEO) is an international, multidisciplinary, peer reviewed, open access journal.

Urban Heat Island mapping based on a Local Climate Zone classification: A case study in Strasbourg city, France.

Nathalia PHILIPPS., Tania LANDERS, Pierre KASTENDEUCH, Georges NAJJAR, Camille GOURGUECHON

Abstracting and Indexing: TR DIZIN, DOAJ, Index Copernicus, OAJI, Scientific Indexing Services, International Scientific Indexing, Journal Factor, Google Scholar, Ulrich's Periodicals Directory, WorldCat, DRJI, ResearchBib, SOBIAD

IJEGEO

International Journal of Environment and Geoinformatics 9(4):057-067 (2022)

Research Article

Urban Heat Island mapping based on a Local Climate Zone classification: A case study in Strasbourg city, France.

Nathalia Philipps1,*, Tania Landes2, Pierre Kastendeuch1, Georges Najjar1, Camille Gourguechon1

[1] Icube Laboratory (UMR 7357), University of Strasbourg, Strasbourg, France
[2] Photogrammetry and Geomatics Group, INSA Strasbourg, CNRS, Icube Laboratory (UMR 7357), Strasbourg, France

* Corresponding author: P. Nathalia
E-mail: nathalia.philipps@etu.unistra.fr

Received 01.03.2022
Accepted 16.03.2022

How to cite: Philipps, et al., (2022). Urban Heat Island mapping using Local Climate Zone classification: A case study in Strasbourg city. *International Journal of Environment and Geoinformatics (IJEGEO)*, 9(4):057-067. doi. 10.30897/ijegeo.1080023

Abstract

The Urban Heat Island (UHI) effect is characterised by higher temperatures in cities than in rural surroundings. This phenomenon leads to increased health risks in urban dwellers, particularly in the context of global climate change. It is essential to consider its spatial variability to propose efficient UHI mitigation strategies. The Local Climate Zone (LCZ) scheme is a climate-based classification that can accurately capture UHI intensities according to the urban area characteristics. In this study, an LCZ classification has been established for the city of Strasbourg by using a vector-based method that relies on a large vector database composed of land cover and cadastral parcels data. LCZ polygons are digitized from cadastral maps, then the different LCZ parameters are calculated for each of them. Six of the ten LCZ parameters proposed in the literature have been obtained. New criteria have been added to improve the classification, i.e. a vegetation parameter (VgSF) and a compactness index (CI). A given LCZ class is then assigned to each polygon using a trapezoidal fuzzy logic model, which is completed by a decision tree. The acquired final LCZ map shows that the developed vector-based method permits obtaining relevant LCZ classification. The LCZ parameters values are subsequently used to determine a multiple linear regression (MLR) aiming to get a UHI intensity for each LCZ polygon. The resulting UHI map of the Eurométropole de Strasbourg (EMS) accurately illustrates the strong spatial heterogeneity of the phenomenon.

Keywords: Urban Heat Island, Local Climate Zone, Multiple Linear Regression, Vector-based method

Introduction

The Urban Heat Island (UHI) effect is defined as the temperature difference between an urban area and its rural surroundings. Its magnitude is commonly greatest after sunset, in particular during calm and clear nights (Oke et al., 2017). This phenomenon has significant implications on public health, air quality, and thermal outdoor comfort, putting additional stress on urban dwellers during heatwave events. It occurs because of the greater heat capacity of building materials, the morphology of the cities, the lack of vegetation, and the high anthropogenic heat release (Arnfield, 2003). Nevertheless, due to the heterogeneous land use and surface characteristics of urban areas, the UHI exhibits an important spatial diversity. As a consequence, the UHI magnitude variability can be conspicuous in a given city (Unger, 2004; Stewart, 2011; Schatz and Kucharik, 2014; Sutariya et al., 2021). In this context, it is essential to investigate the relationships between UHI intensity and urban fabric characteristics to optimize mitigation strategies that will be proposed to urban designers and planners.

As a result of the tremendous urban heterogeneity, many classifications have already been developed to enhance understanding of the urban climate (Chandler, 1965; Ellefsen, 1991; Oke, 2004; Celik et al., 2019). Amongst them, the Local Climate Zone (LCZ) scheme (Stewart and Oke, 2012) uses standardized descriptions of urban and rural landscapes and therefore can be applied in cities all over the world. Each LCZ class is defined by a specific range of geometric and surface-cover values. The LCZ classification consequently enables to identify the main parameters that can strengthen the UHI intensity. Two distinct approaches are commonly used to generate LCZ maps: the raster-based approach and the vector-based approach. The former relies on remote sensing data whereas the latter uses GIS vector layers. Several methods for LCZ mapping have been proposed in the literature (Unger et al., 2014; Bechtel et al., 2015; Geletič and Lehnert, 2016; Sekertekin et al., 2016), each of them with advantages and drawbacks. Although Hidalgo et al., 2019 the LCZ concept was originally designed for urban climate purposes and therefore links UHI magnitude to urban morphology, few previous studies are directly using LCZ parameters to map the phenomenon.

A first raster-based method leading to an LCZ classification for Strasbourg city has been proposed in previous work (Gourguechon, 2018). This method follows the procedure reported in Bechtel et al (2015) and is based on free satellite images (Sentinel-2 or Landsat 8) and the use of free software packages (Google Earth and SAGA GIS). Firstly, training areas are defined for each LCZ. The spectral signature of pixels composing these areas is then compared to reference values of LCZ classes to associate each training area polygon to a given LCZ type. Among the supervised classifier algorithms, the random forest classifier has been chosen since it appears to be an ideal compromise between the achieved accuracy and computational performance according to Bechtel et al (2015). Although this methodology is easily applicable and universal, some biases appear in the process. The approach remains subjective because the training areas are defined by the user and hence depend on its expertise and local knowledge of the given territory. Moreover, it still relies on the quality of remote sensing images that are used. Finally, it only allows reaching the lowest level of detail (L0) from the World Urban Database and Access Portal Tools (WUDAPT). Since the deliverable is limited to the visual information that is provided by remote sensing images, it has been decided to take benefit from vector layers and to develop a vector approach.

This study presents a vector-based method whose aim is to get a more accurate LCZ classification. The associated database and processing chains are described. In this paper, a new method for mapping and assessing the UHI that depends partly on LCZ parameters is also proposed.

Study area

The study area is the whole Eurométropole de Strasbourg (EMS) area, a medium-sized European city (505,000 inhabitants, 339.6 km^2) located in northeastern France (Figure 1). The city has a temperate climate, which can be named Cfb according to the updated Köppen-Geiger classification (Kottek et al., 2006), with warm summers and cold winters. The average annual temperature reaches 10.9°C. July is the warmest month, with a mean monthly maximum temperature of 20.1°C (1981 to 2010 climate normals, Météo France).

Fig. 1. Location of the EMS area (Eurométropole de Strasbourg, France).

Fig. 2. LCZ classification (Stewart and Oke, 2012).

Table 1. LCZ properties (Stewart and Oke, 2012).

Properties	LCZ parameters
Urban morphology	Sky View Factor (SVF) Aspect Ratio (H/W) Height of Roughness Elements (HRE) – [m] Terrain Roughness Class (TRC)
Surface cover	Impervious Surface Fraction (ISF) Pervious Surface Fraction (PSF) Building Surface Fraction (BSF)
Thermal radiative materials properties	Surface albedo Surface admittance -[$J.m^{-2}.s^{-1/2}. K^{-1}$]
Urban metabolism	Anthropogenic heat flux - [$W.m^{-2}$]

Materials and Methods

Description of the database concerning LCZ characteristics

The vector-based method uses precise GIS input data to calculate each contributing factor of the LCZ classification. As mentioned in (Chen et al., 2020), this solution gives a more accurate representation of the LCZ variability. The LCZ classification consists actually of 17 standard LCZ types, among which 10 are considered as "built types" (1-10) and 7 as "land cover types" (A-G) (Figure 2).

The respective values of every one of the 10 physical parameters composing the LCZ determine the class to which each LCZ belongs (Stewart and Oke, 2012). Table 1 presents the LCZ properties and their associated parameters.

Each LCZ class can be thus defined quantitatively by a set of parameter ranges. It is therefore essential to determine these classes as precisely as possible. The raster-based method described above allows reaching only a limited level of precision. Despite that, the subsequent LCZ map (Figure 3) provides interesting results and above all, a first LCZ classification for Strasbourg.

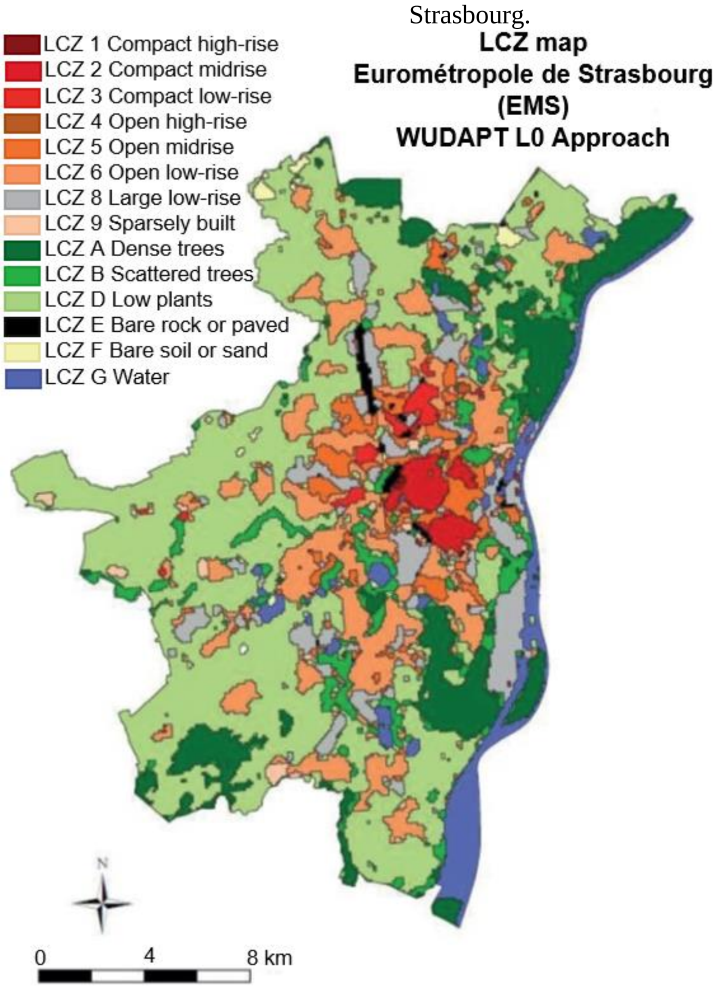

Fig. 3. LCZ classification using a raster-based approach (Gourguechon, 2018).

A high diversity of data is thus required to describe as accurately as possible urban geometry, material properties, land cover surface, vegetation, etc. While the workflow leading to an LCZ classification based on vector data can be generalised, such detailed information is hardly available in all cities in the world and hence prevents the GIS approach from being applied universally. In the case of EMS, a large database composed of many land use and cadastral parcels data is accessible. Free and open data are investigated as a priority so that the methodology is reproducible.

The available dataset is composed of vector and raster data. The former provide elements to define LCZ polygons, while the latter facilitate the determination of LCZ parameters values. These data are collected from several institutes and are composed of fine-resolution images, ranging from some meters to twenty meters, and vector layers for the whole study area.

Determination of LCZ polygons and LCZ parameters

It is essential to check that a given LCZ does not represent mixed urban morphologies and land cover types, otherwise it will only describe a smoothed climate behavior. The cadastral data from our vector database are hence used to digitize polygons which constitute the basic entities of the classification. The layers of these data correspond to either a specific LCZ type or a group of LCZ types.

As mentioned in Hidalgo et al (2019), the polygons can likely fall into four land cover types: built-up areas (LCZ 1-10), vegetated areas (LCZ A-B), agricultural or unbuilt areas (LCZ C-D-F), and water bodies (LCZ G). First, by using GIS tools with ArcMap software, the forest areas and water bodies are linked to their respective land cover types. Only the forest surface areas that are superior to one hectare are investigated, smaller ones would not respect the required LCZ size. Nevertheless, it has been decided to reduce the surface threshold for water bodies to 3000 m^2, otherwise, the main watercourses would have been excluded. The remaining intermediate polygons (also called "islets") are either built areas or agricultural areas. Those having an area superior to one hectare are disjoint from built-up islets. Then the road layers are used to fix agricultural and built islets contours. Industrial and retail areas are classified as built islets whereas agricultural islets are attributed to runways. Finally, those polygons whose area is less than one hectare are merged with their largest contiguous polygon. As a result of the process (Figure 4), 2212 polygons are digitized, with one of the four land cover groups assigned to each of them.

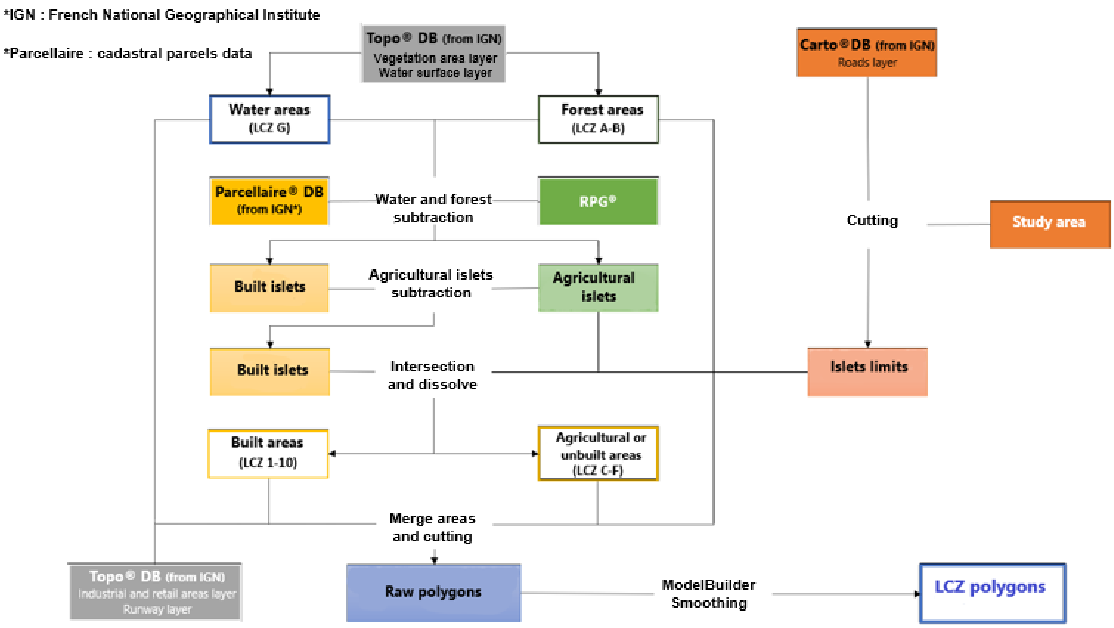

Fig. 4. Methodology used for defining LCZ polygons in the vector based approach.

Based on available data, six of the ten LCZ parameters can be determined, i.e. the Building Surface Fraction (BSF), the Impervious Surface Fraction (ISF), the Pervious Surface Fraction (PSF), the Sky View Factor (SVF), the Height of Roughness Elements (HRE) and the surface albedo, for each polygon.

The surface admittance and the anthropogenic heat flux were omitted due to missing data for the study area. Concerning the two remaining parameters, they were either too difficult to obtain from our data (like the aspect ratio) or had irrelevant results (like TRC).

Classification procedure

Preliminary work must be conducted to exclude the LCZ types which cannot occur in the study area due to local urbanistic and climatic context. This is the case for LCZ 1, since there are no central business districts in Strasbourg, LCZ 7 due to the lack of areas corresponding to slums, and LCZ C because they are mainly located in Mediterranean areas. Up to fourteen LCZ types will thus be potentially distinguished in the final LCZ map of the EMS area.

To assign an LCZ class to each polygon, the fuzzy logic is used, whose application is here a trapezoidal decision rule (Unger et al., 2014). Hence, the membership of polygons to an LCZ type might range between completely true and completely false (Figure 5). If the parameter value belongs to LCZ X ranges, the assigned membership score is equal to 1. Else, the score is between 0 and 1 and proportional to the absolute difference between the parameter value and the closest boundary.

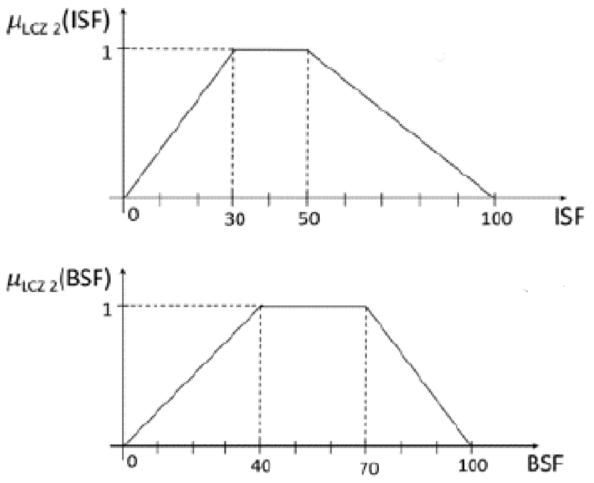

Fig. 5. Fuzzy membership function for ISF and BSF parameters with LCZ 2 class.

Although the trapezoidal membership function tends to follow the four groups described previously, it is not enough to distinguish "built" LCZ types. It is therefore essential to provide additional criteria to better exclude irrelevant LCZ classes. Even if there are neither vegetated surface fraction nor compactness notion in the LCZ scheme, the inclusion of additional parameters should significantly improve the assignment of LCZ classes. Two original parameters were thus added: the Vegetated Surface Fraction (VgSF) and the Compactness Index (CI). The VgSF is calculated as follows:

$$VgSF_{LCZ} = \sum Svege_i/S_{LCZ} \qquad \text{(Eq.1)}$$

Where $Svege_i$ corresponds to an elementary vegetated surface in a polygon i and S_{LCZ} to the total LCZ surface area.

Moreover, the CI takes into account the space between buildings. Actually, the compacter the built zone, the narrower the space between buildings. Thiessen polygons are used to delineate proximal regions around buildings, as shown in Figure 6. The compactness notion is here illustrated with area A which is sparser than area B.

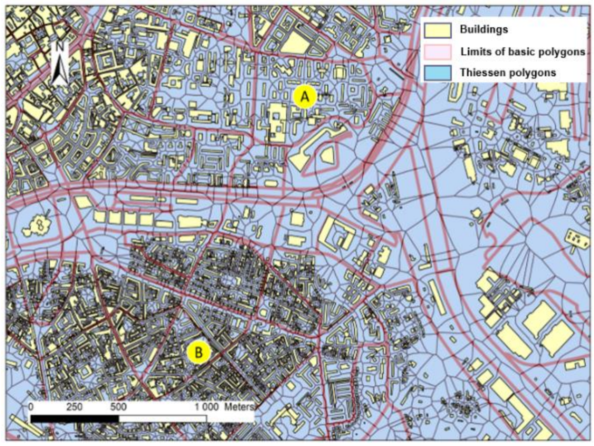

Fig. 6. Compactness index for a part of Strasbourg city based on Thiessen polygons.

As expected, many polygons are still assigned to several LCZ classes. A decision tree inspired by Geletič and Lehnert's study (2016) is therefore introduced to improve the LCZ assignment. It is composed of two main branches: the former follows a succession of tests and decisions that allows attributing the built LCZ class output (LCZ 1-10), whereas the latter does the same but with land cover LCZ types (LCZ A-G). The decision tree relies on the degree of membership and the description of LCZ classes.

Despite improvements in LCZ class assignments, several polygons aren't well-classified yet. It remains difficult to distinguish some LCZ classes from others, due to the lack of some parameters which would provide more information. For example, the LCZ 10 type ("Heavy industry") can't be detected despite the presence of corresponding zones in the EMS area. It results from the lack of anthropogenic heat flux which would allow distinguishing the LCZ 10 class from the LCZ 8 or the LCZ E. Moreover, several outcomes can still result in a given LCZ type.

To better detect some LCZ classes, in particular urban LCZ types, it has been decided to adjust some LCZ parameters values ranges. It permits actually to take into account the urban and regional context, which is here typical for a mid-sized European city. Subsequently, the final decision tree has been adapted to these changes (Figure 7).

Therefore, the developed vector approach and its associated database (Figure 8) are not only used to get a relevant LCZ classification, but also to determine UHI intensities.

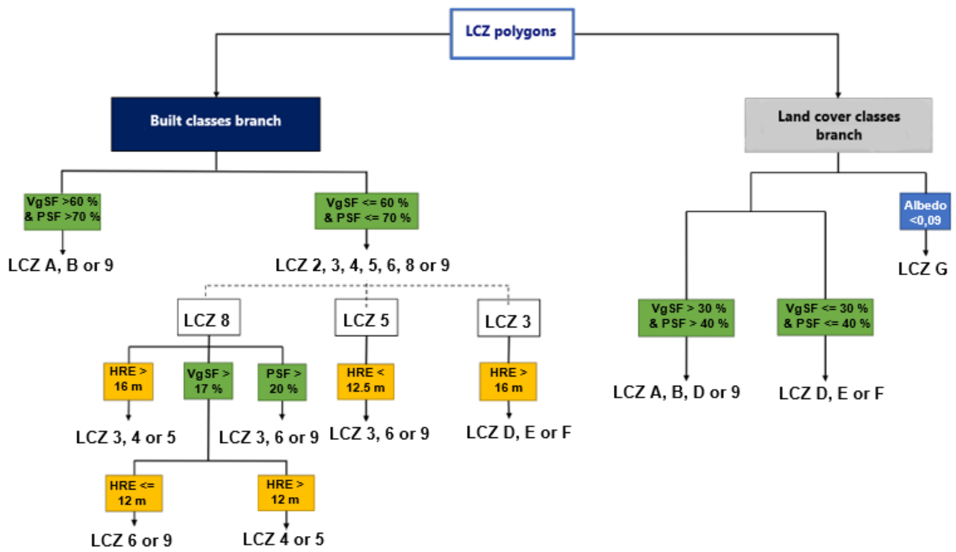

Fig. 7. Final decision tree (Montauban, 2019).

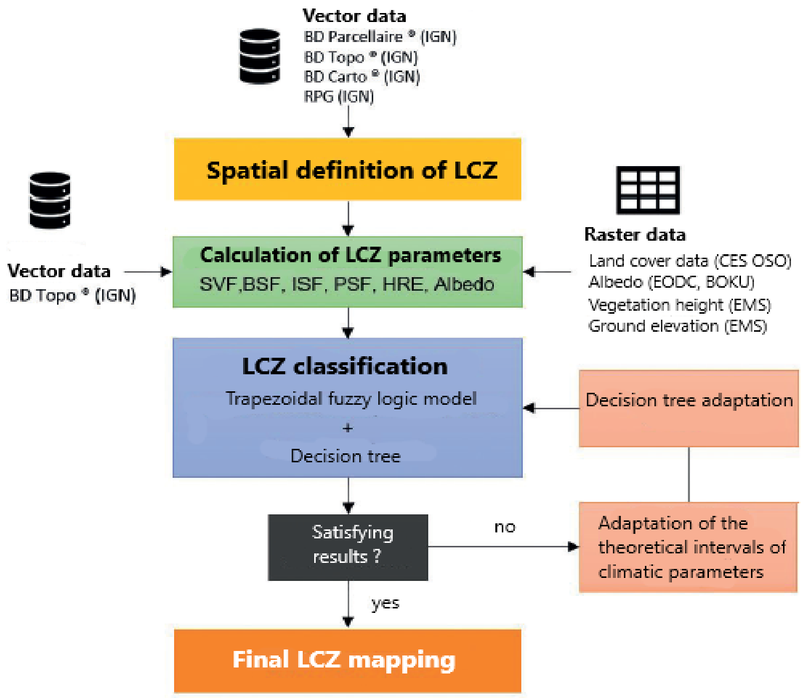

Fig. 8. Diagram of the developed vector-based approach.

Multiple Linear Regression model for UHI mapping

It is well known that LCZ parameters impact UHI intensity, also called ΔTur. In EMS, a network of about twenty weather stations primarily worked between 2013 and 2016 (Philipps et al., 2020). Since the LCZ parameters are henceforth available for each polygon, it is possible to relate them to the ΔTur, and hence to determine a UHI intensity value in any LCZ polygon of the EMS area. Therefore, air temperature data from the meteorological network and the LCZ parameter values of each weather station are used to calculate a multiple linear regression (MLR). The ΔTur in any urban station x at time t is determined by subtracting the air temperature of the rural reference station (here the Entzheim station) from the urban station (Eq. (2)).

$$\Delta Tur_{(x,t)} = Tair\ urban\ station_x - Tair\ rural\ station$$
(Eq.2)

The mean maximum daily ΔTur value of each station is linked with its LCZ parameters values. Several MLR with different LCZ parameters are tested. The BSF, the ISF, and the VgSF, whose respective maps are presented in Figure 9, appear to be the most correlated parameters with the mean ΔTur max (Eq. (3)).

$$0{,}0699 * BSF + 0{,}0572 * ISF - 0{,}0329 * VgSF + 0.3268 = \Delta Tur\ max \qquad \text{(Eq.3)}$$

Equation 3 is then implemented in the SAGA GIS tool and applied to each LCZ polygon to generate a UHI map, as suggested in Bottyan and Unger (2003).

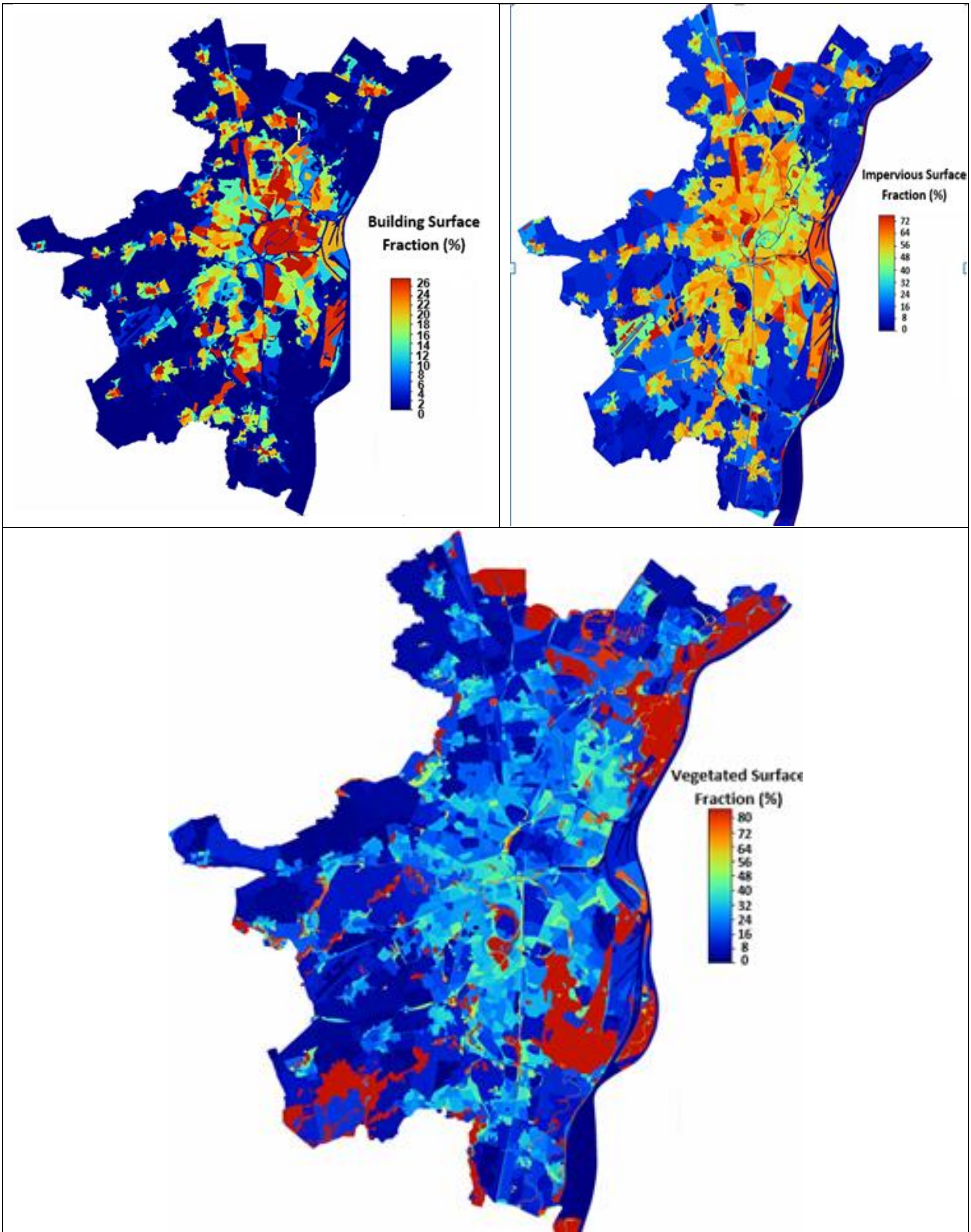

Fig. 9. Maps of (a) Building Surface Fraction (BSF) (b) Impervious Surface Fraction (ISF) and (c) Vegetated Surface Fraction (VgSF).

Results and discussion

The final LCZ classification map

Thirteen LCZ classes out of the seventeen originally defined by Stewart and Oke (2012) were listed for the LCZ classification. Figure 10 presents the resulting classification. It can be noticed that the spatial pattern represents the structure of the EMS area well.

No reference LCZ map exists for the EMS area, so the accuracy of the final LCZ classification map (Figure 10) can't be assessed. However, it has been compared to another LCZ map obtained according to the L0 WUDAPT method (Landes et al., 2020). The results highlight common tendencies, especially concerning the unbuilt LCZ classes repartition. Nevertheless, some differences appear regarding the "built" LCZ types. Firstly, the vector LCZ map is more precise because it integrates height and compactness parameters. Therefore, it allows better distinguishing some urban LCZ classes from others. Secondly, the WUDAPT L0 approach tends to smooth LCZ spatial features whereas the vector approach better captures morphological details. Considering a regular grid composed of 100 m x 100m cells, those containing only one LCZ class are selected and compared between the two approaches. Using a confusion matrix, it can be observed that precision of 91% is achieved, which proves the relevance of the two methods. However, the vector method is more time-consuming compared to the WUDAPT L0 approach, due to the complexity of its implementation. According to the user requirements, it can be advised to use the WUDAPT approach if there is a need only for qualitative analysis. However, if the users need an LCZ map of higher precision for quantitative analysis, the vector approach is recommended.

In addition to this comparative analysis, the LCZ classification has been assessed by experts of the Urban planning and Development Agency of Strasbourg (ADEUS). They validated the classification despite some errors. Their analysis highlights that some areas remain inaccurately classified, in particular urban parks, pitches, graveyards and water bodies shores. These areas are related to the microscale urban structure (several cm to 100m) and can be therefore difficult to assign to an LCZ class since an LCZ might cover hundreds of meters to several kilometers area.

Although the remaining limits, the vector-based LCZ classification can be considered to have reached the L1 WUDAPT level details according to WUDAPT criteria (Bechtel et al., 2015).

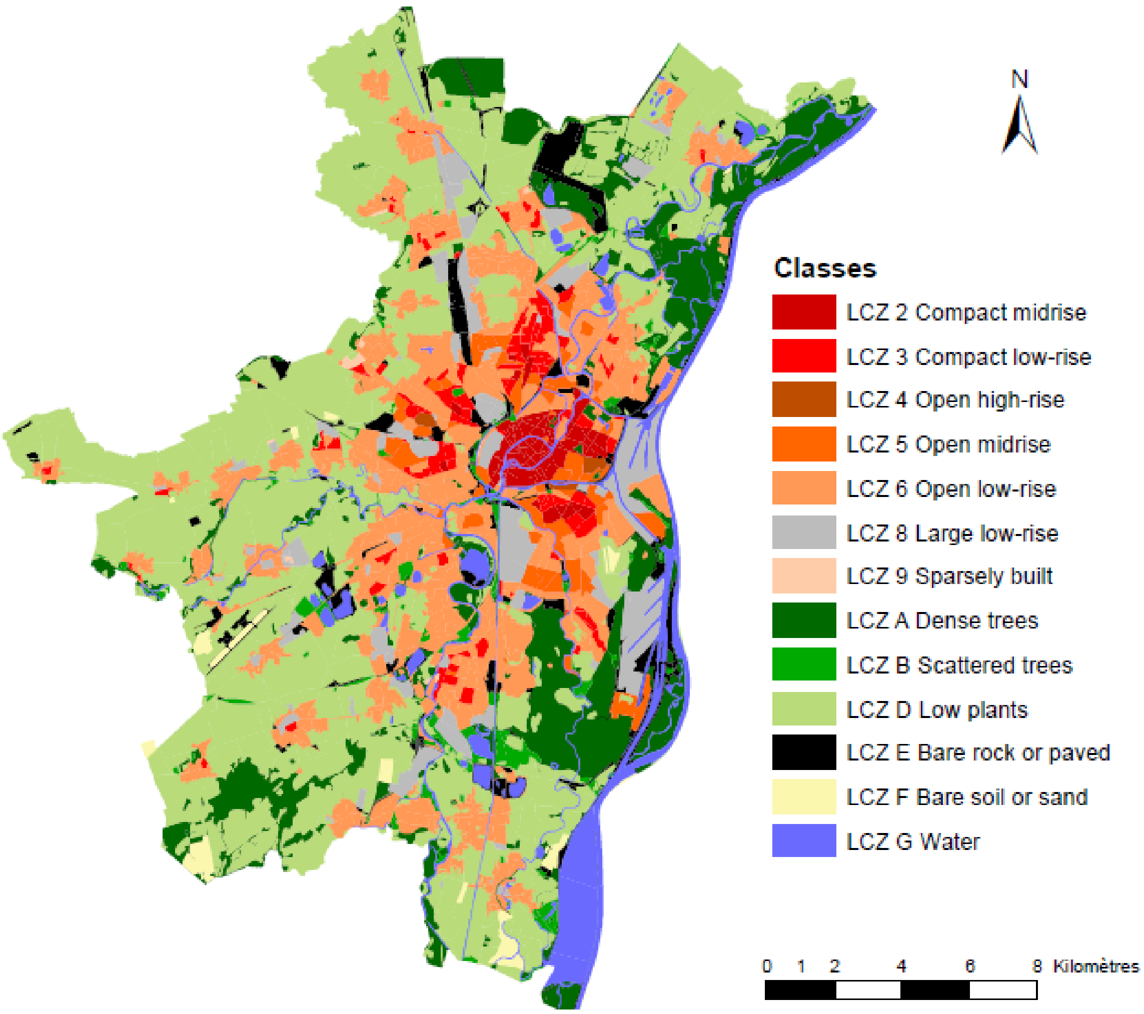

Fig. 10. Final LCZ classification map of the EMS area obtained with the developed vector approach.

UHI map

The methodology described above enables to produce a mean maximum daily UHI map. As it relies on LCZ parameters values of each polygon, its relevance depends simultaneously on the accuracy of the MLR equation and the reliability of the LCZ classification. However, when a polygon has a given LCZ class and its neighbour has another one, very abrupt transitions can occur: some proximal polygons present mean ΔTur max differences of 8°C, which is unrealistic. Therefore, the moving average is applied with SAGA GIS to smooth the obtained UHI intensities.

The final UHI map (Figure 11) presents as expected a strong correlation with the LCZ classification. Calculated mean maximal UHI intensities (ΔTur max) tend to be highest for LCZ 2 and LCZ 3, which characterise the city centre and proximal suburbs. To a lesser extent, some peripheral cities also present stronger UHI intensities in their centre, which is often classified in LCZ 6 or LCZ 8.

The methodology highlights not only the inter-LCZ UHI heterogeneity but also the persistent intra-LCZ variability. For example, the mean ΔTur max values in LCZ 2 vary between 3°C and more than 6°C. Due to their strong BSF value, some urban parks are assigned to LCZ 2 class despite their high VgSF value. The mitigation potential of vegetation on the UHI phenomenon is clearly illustrated here.

Table 2. Performance metrics values for MLR equation.

R^2	Root Mean Square Error (RMSE)	Mean Bias Error (MBE)	Mean Absolute Error (MAE)	Refined index of agreement (dr)
0.71	0.53	-3,21.10^{-16}	0.49	0.99

As shown in Table 2, metrics values show that the MLR model is statistically relevant. However, only twenty ideal weather days in 2015 have been used to average the mean ΔTur max values of the meteorological stations. This is a small sample size and limits the robustness of the model. Besides, some LCZ parameters, like surface albedo, aren't considered in the MLR equation whereas they are also related to UHI intensities.

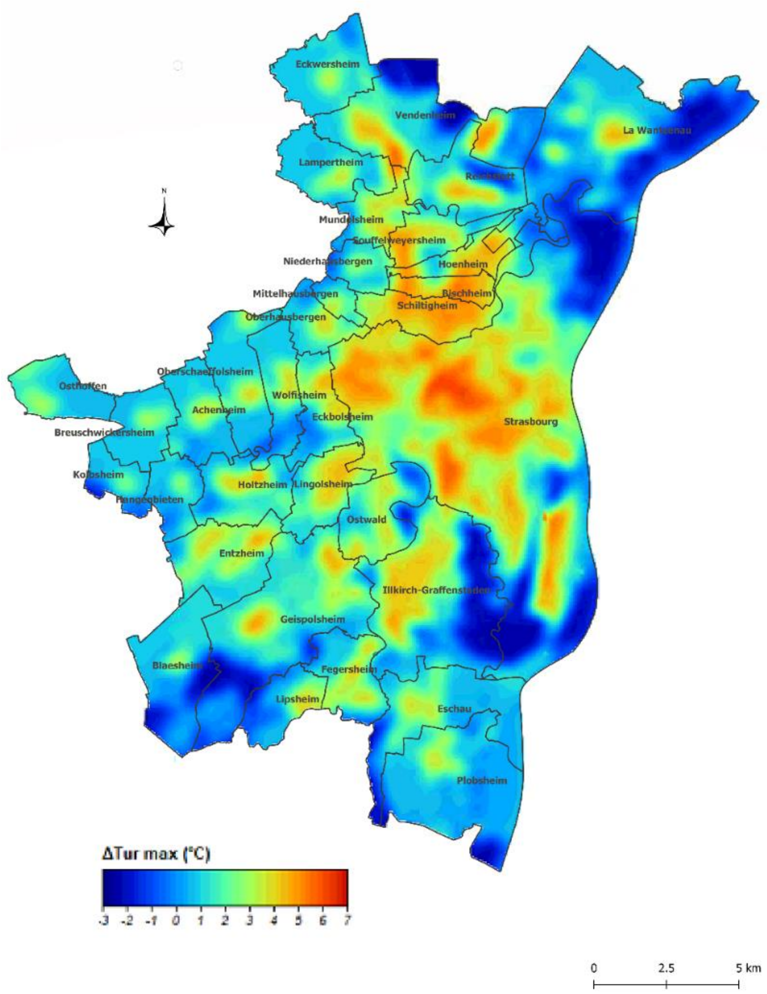

Fig.11. Mean maximum daily UHI intensity map (Philipps et al., 2020).

Conclusion

In this paper, a UHI mapping methodology based on LCZ parameters was developed, as well as the vector approach used to produce the LCZ map of the EMS area. The comparison between the vector-based and the raster-based LCZ classifications showed that both approaches are relevant as they lead to similar LCZ maps. Even though the input data for the vector approach are difficult to acquire and the process is complex and time-consuming, this methodology is more accurate since it relies on more precise and diverse data. As soon as a relevant LCZ classification was available, it was possible to associate LCZ parameters of each LCZ polygon and UHI intensities. This UHI mapping method is easy to apply and permits highlighting the important spatial heterogeneity of the phenomenon as well as the mitigation potential of vegetation. However, this first UHI map still needs to be improved. Although it shows pertinent results which are well correlated to measures, it doesn't include some LCZ parameters, like surface admittance or aspect ratio, which might improve the analysis. Besides, the map illustrates only the mean maximum daily UHI intensity, and neither the mean daily nor the seasonal UHI. Further works will be conducted aiming to produce more significant UHI maps of the EMS area. Finally, some of the remaining LCZ parameters might be calculated as part of future work, which would likely improve the LCZ classification and therefore the UHI mapping.

This study highlights the fact that the UHI analysis depends strongly on the GIS data worldwide available. The study used mainly free data and open-source software to guarantee reproducibility at least in French cities. Actually, the developed methodology is transferable to any city in the world if the necessary input data are available. In the context of future works, the presented UHI map has also been compared to another which was produced by the Meso-NH atmospherical model (Masson, 2000; Lac et al., 2018). Preliminary results show that both maps present noteworthy similarities, which underscores the relevance of the two methods. This will constitute the object of future studies which will be further published.

Acknowledgements

The authors would like to acknowledge the EMS geomatics department for the data of the study area as well as Camille Gourguechon and Olivier Montauban for their precious work made during their Master thesis.

References

Arnfield, A. J. (2003). Two decades of urban climate research: A review of turbulence, exchanges of energy and water, and the urban heat island. *International Journal of Climatology, 23(1)*, 1-26.

Bechtel, B., Alexander, P., Böhner, J., Ching, J., Conrad, O., Feddema, J., Mills, G., See, L., Stewart, I.D. (2015). Mapping Local Climate Zones for a worldwide database of the form and function of cities. *ISPRS International Journal of Geoinformation, 4(1)*, 199-219.

Bottyan, Z., Unger, J. (2003). A multiple statistical linear model for estimating the mean maximum urban heat island. *Theoretical and Applied Climatology, 75*, 233-243.

Celik, B., Kaya, Ş., Alganci, U., Seker, DZ. (2019). Assessment of the relationship between land use/cover changes and land surface temperatures: a case study of thermal remote sensing, FEB Fresenius Environ. Bull.,3, 541

Chandler, T.J. (1965). The Climate of London. Hutchinson.

Chen, Y., Zheng, B., Hu, Y. (2020). Mapping Local Climate Zones using ArcGIS-based method and exploring Land Surface Temperature characteristics in Chenzou, China. *Sustainability, 12*, 2974.

Ellefsen, R. (1991). Mapping and measuring buildings in the urban canopy boundary layer in ten US cities. *Energy and Buildings, 15-16*, 1025-1049.

Geletič, J., Lehnert, M. (2016). GIS-based delineation of local climate zones: The case of medium-sized Central European cities. *Moravian Geographical Reports, 24(3)*, 2-12.

Gourguechon, C. (2018). Classification de données images et vecteur et de nuages de points dans le but d'extraire des zones climatiques types dans des quartiers de Strasbourg. *Technological research project*, INSA Strasbourg, France. http://eprints2.insa-strasbourg.fr/3266/

Hidalgo, J., Dumas, G., Masson, V., Petit, G., Bechtel, B., Bocher, E., Foley, M., Schoetter, R., Mills, G. (2019). Comparison between local climate zones maps derived from administrative datasets and satellite observations. *Urban Climate, 27*, 64-89.

Kottek, M., Grieser, J., Beck, C., Rudolf, B., Rubel, F. (2006). World map of the Köppen-Geiger climate classification updated. *Meteorologische Zeitschrift, 15*, 259-263.

Lac, C., Chaboureau, J.-P., Masson, V., Pinty, J.-P., Tulet, P., et al. (2018). Overview of the Meso-NH model version 5.4 and its applications. *Geoscientific Model Development, 11*, 1929-1969.

Landes, T., Najjar, G., Koehl, M., Montauban, O., Gourguechon, C., Kastendeuch, P., Slisse, P. (2020). Création de cartes de zones climatiques locales pour le suivi des îlots de chaleur urbains à Strasbourg. *Revue XYZ de l'Association Française de Topographie (AFT), 163*, 53-61.

Masson, V. (2000). A physically-based scheme for the urban energy budget in atmospheric models. *Boundary-layer Meteorology*. 118, 477-501.

Oke, T.R. (2004). Initial guidance to obtain representative meteorological observations at urban sites. IOM Rep. 81, World Meteorological Organization/TD-No 1250.

Oke, T.R., Mills, G., Christen, A., Voogt, J.A. (2017). Urban climates. Cambridge University Press.

Philipps, N., Kastendeuch, P.P, Najjar G. (2020). Analyse de la variabilité spatio-temporelle de l'ICU strasbourgeois. *Climatologie*, *17*, 10.

Schatz, J., Kucharik, C.J. (2014). Seasonality of the urban heat island effect in Madison, Wisconsin. *Journal of Applied Meteorology and Climatology, 53(10)*, 2371-2386.

Sekertekin, A., Kutoglu, S.H.; Kaya, Ş. (2016). Evaluation of spatio-temporal variability in land surface temperature: A case study of Zonguldak, Turkey. Environ. Monit. Assess, 188, 30.

Stewart, I.D. (2011). A systematic review and scientific critique of methodology in modern urban heat island literature. *International Journal of Climatology*, *31(2)*, 200-217.

Stewart, I.D., Oke, T.R. (2012). Local Climate Zones for urban temperature studies. *Bulletin of the American Meteorological Society, 93,* 1879-1900.

Sutariya, S., Hirapara, A., Meherbanali, M., Tiwari, M., Sıngh, V., Kalubarme, M. (2021). Soil Moisture Estimation using Sentinel-1 SAR Data and Land Surface Temperature in Panchmahal District, Gujarat State. *International Journal of Environment and Geoinformatics*, 8(1), 65-77.doi.10.30897/ijegeo.777434

Unger, J. (2004). Intra-urban relationship between surface geometry and urban heat island: review and new approach. *Climate Research, 27(3)*, 253-264.

Unger, J., Lelovics, E., Gál, T. (2014). Local climate zone mapping using GIS methods in Szeged. *Hungarian Geographical Bulletin, 63(1)*, 29-41.